The application of a transformational zone method to the calculation of radiation heat transfer inside a piston-cylinder system

M. W. Collins and J. Stasiek*
Thermo-Fluids Engineering Research Centre, City University, London, UK

A radiation heat transfer analysis has been formulated for the space inside an internal combustion engine cylinder using the principles of the Hottel zone and transformational zone methods. The space analyzed has a variable length resulting from the piston movement. The analysis presented here is for radiation in piston-cylinder systems of known temperatures of radiation gas, and internal surfaces of cylinder, head, and piston. Radiative emissions of the radiation gas in the shape of rings were determined on the basis of Stasiek's principle of surface transformation. The results obtained demonstrate the present approach satisfactorily, both qualitatively and quantitatively. Moreover, the division of the analyzed volume into infinitely small elements along the axial direction has significantly simplified the calculations in comparison with the conventionally employed classical Hottel zone method.

Keywords: radiation heat transfer; transformational zone method; piston-cylinder system; theoretical analysis

Introduction

The prediction of the thermal performance of fossil-fueled energy units, such as furnaces and combustion chambers, is dependent on an accurate calculation of radiant exchange between the combustion products, walls, and head within the heating or cooling chamber. It often involves the analysis of convective and radiative transfer in a cylindrical system. This may be based on solutions of the governing integrodifferential equations, which use exponential wide-band models,[4,5] flux methods,[7] two-flux spherical harmonics methods,[14] or zone methods.[10,11,17–20] The zone method has a wide range of application to energy generation systems, exhibits an ability to predict real gas behavior in multidimensional systems, and has been successfully employed to examine temperature distributions and heat transfer rates in furnaces and circular enclosures.[10,17,19,20] It has been applied in the present study.

This paper reports an analysis of the radiation heat transfer inside a combustion engine cylinder of a variable length resulting from the piston movement. With respect to an arbitrary location of the piston, the volume under consideration is divided radially into a finite number of rings but axially into infinitely small elements. The rings of axial thickness dX obtained in this way are characterized by appropriate radiative properties that can vary depending on the successive positions of the piston.

The current analysis deals with radiation heat transfer in a combustion engine cylinder of a known initial temperature field of the radiation gas and the internal surfaces of cylinder, head, and piston. The emissions of the radiation gas volumes in the shape of rings were determined on the basis of Stasiek's[21–23] principle of surface transformation. The division of the volume under consideration into infinitely small axial elements of surface and volume leads to a differential equation describing in a continuous way the heat flux on the cylinder wall (liner). Calculation of the heat fluxes was possible from the experimental data and was carried out for various piston positions and emissions of cylinder walls and the radiation gas.

The proposed method makes it possible to determine the maximum heat fluxes on the walls in a pseudodynamic manner, i.e., the assumption of instantaneous thermodynamic equilibrium is made. This is consistent with the quasi-steady thermodynamic-based models discussed by Heywood and Cohen[8] and Wisniewski.[25] The calculated results presented justify both quantitatively and qualitatively the theoretical approach and, moreover, the division of the volume analyzed into infinitely small axial elements has significantly simplified the calculations in comparison with the classical Hottel zone method. Although the analysis presented is for pure radiation, it would be a straightforward development to include convection effects, which can be accommodated in a fairly comprehensive manner.

Theoretical analysis

The system to be analyzed is shown schematically in Figure 1. An optically active medium (i.e., radiation gas) at a specified temperature profile flows into the tube under steady-state conditions. The cylinder wall is cooled on the outside with a nonuniform heat flux $q_R(X)$. The outer surfaces of the piston-cylinder system (head and piston) are perfectly insulated

* On leave of absence from Technical University of Gdansk, Poland.

Address reprint requests to Professor Collins at the Thermo-Fluids Engineering Research Centre, City University, London, EC1V 0HB, UK.

Received 18 September 1989; accepted 30 December 1991

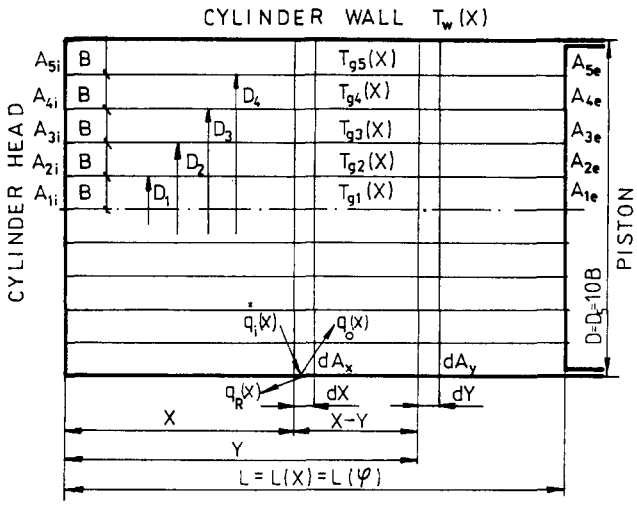

Figure 1 Schematic diagram of piston-cylinder system

and black ($\varepsilon_i = \varepsilon_e = 1$), and each of them has a temperature profile: $T_{i,i}(r)$ for head and $T_{i,e}(r)$ for piston. The inner surface of the liner is diffuse-gray of emissivity ε. The radiation gas absorbs and emits thermal radiation with temperature and pressure (i.e., path length) dependent radiative properties described by the weighted sum of a gray gases model[4,8,18] and soot flame radiation.[8,15] Axial and radial conduction within the gas and duct wall are assumed to be negligible. It is also assumed that the Planck mean volume absorption coefficient α is constant for each position of the piston given by $L = L(X)$ and the optical thickness $\kappa(S) \ll 1$. The nonisothermal gray gas is divided along the axis into elementary (infinitely small) sections each of length dX. Each of these sections is divided into (in this case) five coaxial cylindrical rings in such a way that the radius of the innermost cylinder shell and the distance between one cylinder shell and the next are equal and constant with value B. The apparent emissivity of the radiation gas in the form of an elementary ring is assumed to be as for a circular slice, giving a shape factor Z of 1.5.[21,22] Calculations were also made for $Z = 2.0$.

Energy balance

An analytical relation between temperatures and heat fluxes can be obtained from an energy balance on an elementary surface dA. According to the net-radiation method of Poljak[30] and other work[13,21,22] the energy balance for an elementary surface of wall dA_x a distance X from the cylinder head is written as

$$q_R(X) = q_i^*(X) - q_0(X) \tag{1}$$

where

$q_R(X)$ = outward heat flux from surface element (wall heat flux)
$q_i^*(X)$ = radiative heat flux incident on surface element
$q_0(X)$ = radiative heat flux leaving surface element

In Equation 1 according to Siegel and Howell,[15] Perlmutter and Siegel,[13] and Stasiek[22,23] the radiative heat fluxes leaving a surface element are calculated as follows:

$$q_0(X) = \varepsilon\sigma T_w^4(X) + (1-\varepsilon)q_i^*(X) \tag{2}$$

The incident radiative flux on the elementary surface $q_i^*(X)$ consists of three components:

- the radiation incoming from the five surfaces of the cylinder, head, and piston;

Notation

A	Area or constant of Equation 22
B	Constant of Equation 22
C	Constant of Equation 21
D	Cylinder diameter
E	Energy emitted per unit time
e	Emissive power
F	Geometric configuration factor, Appendix 1
f	Free term in Equation 14
H	Enthalpy flux
K	Geometric configuration factor between elements on inside of cylinder wall or constant
k	Dimensionless radiation gas absorption coefficient
L	Length of cylinder wall
l	Dimensionless length
m	Modulus of Equation 14
n	Refractive index
q	Heat added per unit area and time
Q	Heat flux
R_i, R_e	Short record, Equations 20a and 20b
R	Radius of a circle
S	Coordinate along path of radiation
T	Temperature
t	Dimensionless temperature
V	Volume
X	Axial length coordinate measured from cylinder geometry
x	Dimensionless coordinate
Y	Dummy integration variable
y	Dimensionless heat added per unit area
Z	Shape factor

Greek symbols

α	Absorption coefficient
ε	Emissivity of surface
$d(\varepsilon_{p,i})$	Apparent emissivity of radiation gas body*
ξ	Dimensionless dummy integration variable
$\kappa(S)$	Optical thickness of layer of thickness S
κ	Extinction coefficient
σ	Stefan-Boltzmann constant or scattering coefficient
τ	Transmissivity

Subscripts

b	Black body
e	Surface of piston
g	Gas
i, j	Surface of cylinder head or number of volume zones with radial and axial width
m	m of surfaces
R	Radiant
n	n of volumes
s	Scatter
w	Wall

* Following Siegel and Howell[15] we have used the term *radiation gas* for one with an absorbing, emitting, and scattering medium.

- the radiation arriving as a result of the outward radiation from the other elements of the internal cylinder wall;
- the radiation arriving from the elementary cylinder shell rings.

These quantities can be written, respectively, as

$$q_i^*(X) = \sigma\tau(X)\sum_{i=1}^{i=5} T_{i,i}^4 F_{dX-i,i}(X) + \sigma\tau(L-X)\sum_{i=1}^{i=5} T_{i,e}^4 F_{dX-i,e}(L-X) + \int_0^X q_0(Y)dF_{dY-dX}(X-Y)\tau(X-Y) + \int_X^L q_0(Y)dF_{dY-dX}(Y-X)\tau(Y-X) + \sigma\sum_{i=1}^{i=5}\left[\int_0^X T_{g,i}^4(Y)d(\varepsilon_{p,i})F_{dX-Y,i}(X-Y)\tau(X-Y) + \int_X^L T_{g,i}^4(Y)d(\varepsilon_{p,i})F_{dX-Y,i}(Y-X)\tau(Y-X)\right] \quad (3)$$

Equation 3 has been derived by making use of reciprocal configuration and the principle of enclosure.[2,15,21] After appropriate combination of Equations 1–3 we obtain a relation between q_R, T_w, and T_g as follows:

$$q_R(X) - (1-\varepsilon)\left[\int_0^X q_R(Y)dF_{dY-dX}(X-Y)\tau(X-Y) + \int_X^L q_R(Y)dF_{dY-dX}(Y-X)\tau(Y-X)\right] + \varepsilon\sigma T_w^4(X) = \varepsilon\sigma\left[\tau(X)\sum_{i=1}^{i=5} T_{i,i}^4 F_{dX-i,i}(X-Y) + \tau(L-X)\sum_{i=1}^{i=5} T_{i,e}^4 F_{dX-i,e}(L-X)\right] + \varepsilon\sigma\left[\int_0^X T_w^4(Y)dF_{dY-dX}(X-Y)\tau(X-Y) + \int_X^L T_w^4(Y)dF_{dY-dX}(Y-X)\tau(Y-X)\right] + \varepsilon\sigma\sum_{i=1}^{i=5}\left[\int_0^X T_{g,i}^4(Y)d(\varepsilon_{p,i})dF_{dX-Y,i}(X-Y)\tau(X-Y) + \int_X^L T_{g,i}^4(Y)d(\varepsilon_{p,i})dF_{dX-Y,i}(Y-X)\tau(Y-X)\right] \quad (4)$$

Equation 4 permits the calculation of the wall heat flux from the surface element for a specified position of piston L, emissivity values for the liner internal surface ε, and the radiation gas and liner temperature fields.

We now introduce dimensionless quantities defined by

$$x = \frac{X}{D}; \quad \xi = \frac{Y}{D}; \quad l = \frac{L}{D}; \quad k = \alpha D; \quad dx = \frac{dX}{D}; \quad d\xi = \frac{dY}{D} \quad (5)$$

and appropriate values of the magnitudes that appear in Equation 4, namely[21–23]

$$dF_{dY-dX}(X-Y) = K(X-Y)dX \quad (6)$$

$$dF_{dY-dX}(Y-X) = K(Y-X)dX \quad (7)$$

$$\tau(X) \cong e^{-\alpha X}; \quad \tau(L-X) \cong e^{-\alpha(L-X)} \quad (8)$$

$$d(\varepsilon_{p,i}) = Z\alpha_i dX \quad (9)$$

$$F_{dX-Y,i}(X-Y) = F_{Y,i}(X-Y); \quad F_{dX-Y,i}(Y-X) = F_{Y,i}(Y-X) \quad (10)$$

$$F_{dX-i,i}(X) = F_{i,i}(X); \quad F_{dX-i,e}(L-X) = F_{i,e}(L-X) \quad (11)$$

$$K(X) \cong e^{-2X}; \quad K(L-X) \cong e^{-2(L-X)} \quad (12)$$

Hence the following equation for $q_R(X)$ is obtained from Equation 4

$$q_R(x) - (1-\varepsilon)\left[e^{-(2+k)x}\int_0^x q_R(\xi)e^{(2+k)\xi}d\xi + e^{(2+k)x}\int_x^l q_R(\xi)e^{-(2+k)\xi}d\xi\right] + \varepsilon\sigma T_w^4(x) = \varepsilon\sigma\left\{e^{-kx}\sum_{i=1}^{i=5} T_{i,i}^4 F_{i,i}(x) + e^{-k(l-x)}\sum_{i=1}^{i=5} T_{i,e}^4 F_{i,e}(l-x) + e^{-(2+k)x}\int_0^x T_w^4(\xi)e^{(2+k)\xi}d\xi + e^{(2+k)x}\int_x^l T_w^4(\xi)e^{-(2+k)\xi}d\xi + Zk\sum_{i=1}^{i=5}\left[e^{-kx}\int_0^x T_{g,i}^4(\xi)F_{Y,i}(x-\xi)e^{k\xi}d\xi + e^{kx}\int_x^l T_{g,i}^4(\xi)F_{Y,i}(\xi-x)e^{-k\xi}d\xi\right]\right\} \quad (13)$$

Transformation to a differential equation

Integral-differential equations can be treated by applying various methods.[15] In this paper the method used is of differentiating the initial equations to be transformed, so that the original differential-integral form is replaced by a differential one.

By differentiating Equation 13 twice and then transforming with a simultaneous application of relationships for approximate values of the configuration coefficients (specified in Appendix 1), it is possible to obtain from Equation 13 the following differential equation in a dimensionless form:

$$\frac{d^2y}{dx^2} - m^2y = f(x) \quad (14)$$

where

$$y = \frac{q_R(x)}{q}; \quad m = \sqrt{[K^2 - 2K(1-\varepsilon)]} \quad (15, 16)$$

$$f(x) = \frac{F(x)}{q} = \varepsilon Kkt_w^4 - \varepsilon\left[12t_w^2\left\{\frac{dt_w}{dx}\right\}^2 + 4t_w^3\frac{d^2t_w}{dx^2}\right] - 2ZK\varepsilon R_i \quad (17)$$

$$K = (2+k); \quad t = T\left\{\frac{\sigma}{q}\right\}^{1/4} \quad (18)$$

In the above, q has an arbitrary constant value (for instance $q_R(0)$), which will be attached later (see below).

Boundary conditions

The boundary conditions for Equation 14 are found from the integral Equation 13 by evaluating it at two points. Two convenient conditions are those at the beginning and end of the piston cylinder.

at $x = 0$

$$\left.\frac{dy(0)}{dx}\right|_{x=0} = Ky(0) + K\varepsilon t_w^4(0) - 4\varepsilon t_w^3(0)\frac{dt_w(0)}{dx} - 2K\varepsilon R_i \tag{19}$$

and for $x = l$

$$y(l) - (1-\varepsilon)e^{-Kl}\int_0^l y(\xi)e^{K\xi}d\xi = \varepsilon\left\{-t_w^4(l) + e^{-Kl}R_i + R_e + Zk\left[\frac{e^{-Kl}}{32}\int_0^l t_{g,1}^4(\xi)e^{K\xi}d\xi + \frac{e^{-Kl}}{10}\int_0^l t_{g,2}^4(\xi)e^{K\xi}d\xi + \frac{e^{-Kl}}{8}\int_0^l t_{g,3}^4(\xi)e^{K\xi}d\xi + \frac{e^{-Kl}}{4}\int_0^l t_{g,4}^4(\xi)e^{K\xi}d\xi + \frac{e^{-Kl}}{6}\int_0^l t_{g,5}^4(\xi)e^{K\xi}d\xi\right] + e^{-Kl}\int_0^l t_w^4(\xi)e^{K\xi}d\xi\right\} \tag{20}$$

where

$$R_i = \frac{t_{1,i}^4}{32} + \frac{t_{2,i}^4}{10} + \frac{t_{3,i}^4}{8} + \frac{t_{4,i}^4}{4} + \frac{t_{5,i}^4}{6} \tag{20a}$$

$$R_e = \frac{t_{1,e}^4}{32} + \frac{t_{2,e}^4}{10} + \frac{t_{3,e}^4}{8} + \frac{t_{4,e}^4}{4} + \frac{t_{5,e}^4}{6} \tag{20b}$$

where the approximation 8 and 12, and configuration factors from Appendix 1, have been used for τ, K, and F. The procedure, which yields boundary conditions 19 and 20, is presented in Siegel and Howell,[15] Perlmutter and Siegel,[13] and Stasiek,[21-23] although, for each trial solution a value for $y(0)$ is approximated. Since the Equation 13 at $x = 0$ has been used to derive Equation 19, this boundary condition is automatically satisfied by using the constants C_1 and C_2 defined by Equation 21 for each trial value of $y(0)$ and we have only to satisfy condition 20. This condition will be satisfied when the correct value for $y(0)$ is found by interpolating over several trials.[13,15,21]

Analytical investigations

A general solution of the differential Equation 14 is the sum of solutions of a homogeneous and of a particular equation. If the solution of the homogeneous equation can be presented in the following form:

$$y = C_1\exp(mx) + C_2\exp(-mx) \tag{21}$$

the solution of the particular Equation 14 depends on the form of the free term $f(x)$. In this work, treating $f(x)$ takes into consideration the substantial magnitudes of the temperature field occurring during a specific operation cycle of a given combustion cylinder. The dimensions are piston diameter $D = 100$ mm, $L = 120$ mm, and stroke $s = 100$ mm ($x = 0.2$–1.2). The quoted values from Wisniewski,[25] Heywood and Cohen,[8] and Woschni and Fieger[28] in Table 1, refer to the surface temperatures of the head and the piston, the internal cylinder surface, and the exhaust smoke. The temperature distributions of the cylinder internal surface and the smoke have been approximated in terms of exponential functions and expressed in a dimensionless form assuming that $q = 10{,}000$ W/m^2. Of course, it is worth stressing here that q is arbitrary, and any desired value may be attached to it.

According to the data given in Table 1, the free term $f(x)$ defined by Equation 17 takes the form:

$$f(x) = \sum_{i=1}^{6} A_i\exp(-B_ix) \tag{22}$$

where

$$A_1 = \varepsilon[Kk - 16\alpha^2]t_w^4(0); \qquad B_1 = 1.6 \tag{23}$$

$$A_2 = -\tfrac{1}{16}ZKk\varepsilon t_{g,i}^4(0); \qquad B_2 = 3.2 \tag{24}$$

$$A_3 = -\tfrac{1}{5}ZKk\varepsilon t_{g,2}^4(0); \qquad B_3 = 3.16 \tag{25}$$

$$A_4 = -\tfrac{1}{4}ZKk\varepsilon t_{g,3}^4(0); \qquad B_4 = 3.16 \tag{26}$$

$$A_5 = -\tfrac{1}{2}ZKk\varepsilon t_{g,4}^4(0); \qquad B_5 = 3.2 \tag{27}$$

$$A_6 = -\tfrac{1}{3}ZKk\varepsilon t_{g,5}^4(0); \qquad B_6 = 3.28 \tag{28}$$

It has been assumed according to the form of Equation 22 that the numerical values of coefficients B_i are not roots of a homogeneous equation. Thus, the solution of Equation 14 can be presented in the following way:

$$y = \sum_{i=1}^{6}\frac{A_i}{(B_i^2 - m^2)}\exp(-B_ix) + C_1\exp(mx) + C_2\exp(-mx) \tag{29}$$

Then, using Equations 29 and 19, it is possible to determine constants C_1 and C_2 with the assumption that for $x = 0$ $y(x) = y(0)$. These are obtained as

$$C_1 = \frac{1}{2m}\left\{y(0)[K+m] + t_w^4(0)[K\varepsilon + 4\alpha\varepsilon] - 2K\varepsilon R_i + \sum_{i=1}^{6}\frac{(B_i - m)}{(B_i^2 - m^2)}A_i\right\} \tag{30}$$

Table 1 Experimental temperature data for a given piston-cylinder arrangement[8,25,28]

$T_w(0)$	551K	T_w (551 ↔ 369K)	369K	$T_w(l)$
$t_w(0)$	0.85	$t_w = 0.85\exp - 0.4x = t_w(0)\exp -\alpha x$	0.525	$t_w(l)$
$T_{5,i}$	550K	$T_{g,5}$ (1,700 ↔ 750K)	570K	$T_{5,e}$
$t_{5,i}$	0.849	$t_{g,5} = 2.623\exp -0.82x = t_{g,5}(0)\exp -\beta_5x$	0.880	$t_{5,e}$
$T_{4,i}$	650K	$T_{g,4}$ (1,900 ↔ 850K)	600K	$T_{4,e}$
$t_{4,i}$	1.003	$t_{g,4} = 2.932\exp -0.8x = t_{g,4}(0)\exp -\beta_4x$	0.926	$t_{4,e}$
$T_{3,i}$	800K	$T_{g,3}$ (2,200 ↔ 1,000K)	620K	$T_{3,e}$
$t_{3,i}$	1.235	$t_{g,3} = 3.395\exp -0.79x = t_{g,3}(0)\exp -\beta_3x$	0.957	$t_{3,e}$
$T_{2,i}$	650K	$T_{g,2}$ (2,100 ↔ 950K)	650K	$T_{2,e}$
$t_{2,i}$	1.003	$t_{g,2} = 3.241\exp -0.79x = t_{g,2}(0)\exp -\beta_2x$	1.003	$t_{2,e}$
$T_{1,i}$	600K	$T_{g,1}$ (2,000 ↔ 900K)	650K	$T_{1,e}$
$t_{1,i}$	0.926	$t_{g,1} = 3.086\exp -0.8x = t_{g,1}(0)\exp -\beta_1x$	1.003	$t_{1,e}$

$$C_2 = -\frac{1}{2m}\left\{y(0)[K-m] - t_w^4(0)[K\varepsilon + 4\alpha\varepsilon] + 2K\varepsilon R_i + \sum_{i=1}^{6}\frac{(B_i+m)}{(B_i^2-m^2)}A_i\right\} \quad (31)$$

The boundary condition for $x = l$ is appropriately transformed to relationship 32.

$$\begin{aligned} y(l) - (1-\varepsilon)e^{-Kl}&\left\{\sum_{i=1}^{6}\frac{A_i}{(K-B_i)(B_i^2-m^2)} \times [\exp(K-B_i)l - 1] \right. \\ &+ \frac{C_1}{(K+m)}[\exp(K+m)l-1] + \frac{C_2}{(K-m)} \left. \times [\exp(K-m)l - 1]\right\} \\ = \varepsilon&\left[-t_w^4(0)\exp(-B_1 l) + \exp(-Kl)R_i + R_e \right. \\ &+ Zk\exp(-Kl)\left\{\frac{t_{g,i}^4(0)}{32(K-B_2)}[\exp(K-B_2)l-1] \right. \\ &+ \frac{t_{g,2}^4(0)}{10(K-B_3)}[\exp(K-B_3)l-1] \\ &+ \frac{t_{g,3}^4(0)}{8(K-B_4)}[\exp(K-B_4)l-1] \\ &+ \frac{t_{g,4}^4(0)}{4(K-B_5)}[\exp(K-B_5)l-1] \\ &\left.+ \frac{t_{g,5}^4(0)}{6(K-B_6)}[\exp(K-B_6)l-1]\right\} \\ &\left.+ \frac{t_w^4(0)}{(K-B_1)}\exp(-Kl)[\exp(K-B_1)l-1]\right] \end{aligned} \quad (32)$$

It is then necessary to solve Equation 29, i.e., to determine the dimensionless heat flux on the cylinder wall (liner) $y(x)$ as a function of the local piston position (determined by the dimensionless length l). The procedure is based primarily on the temperature field assumption (here we are using exponential relations), dimensionless absorption coefficient k, assumption of preliminary value $y(0)$ for $x = 0$, and calculation of C_1 and C_2. Having determined the distribution of the dimensionless heat flux $y(x)$ from Equation 29, it is then necessary to satisfy the relationship given by Equation 32. The iterative process is carried out until an appropriate convergence of the solution is obtained.

Calculated results and discussion

The heat transfer between a radiation gas and internal piston-cylinder surfaces is predominantly by forced convection and radiation. The proportions of the two modes differ considerably between spark-ignition and compression-ignition engines. In the former, homogeneous combustion proceeds entirely in the gaseous phase, and radiation is correspondingly limited. Although the latter may reach about 20 percent of the total transfer within the cylinder, it is commonly subsumed into the convective transfer by adjustment of the appropriate coefficient.[8,25,26] In the compression-ignition (diesel) engine, on the other hand, heterogeneous combustion necessarily proceeds through a stage in which soot flame particles are produced, and the radiation from these is strong. For a long time, the radiant heat transfer was considered to be a small proportion of the total heat transfer in accordance with the estimate provided by Nusselt's equation for calculating the heat transfer rate.[8,12,25] More recently, however, it has become increasingly accepted that radiant heat transfer is important in diesel engines. For example, Butler (William Doxford Co., UK) predicted that the radiation component would account for 75 percent of the total heat transfer in very large (marine) diesel engines of 1,000-mm bore.[12] The radiation from soot particles in the diesel engine flame has been shown to be about five times that from the gaseous combustion products.[8,25,26]

Research on heat transfer in internal combustion engines has been made by various pioneers and is still being pursued. Results are given in numerous research papers.[1,3,6,8,12,16,25,26,28] Recently, Alkidas and Myers,[1] Dent and Sulaiman,[3] Flynn *et al.*,[6] Oguri and Inaba,[12] and Heywood and Cohen[8] presented the results of local measurements of radiative heat flux and the radiation intensity of flame soot as a function of load conditions, crank angle, engine boost pressure and speed, speed fueling, etc. In the measurements of Flynn *et al.*[6] peak equivalent gray-body emissivities around 0.8 ~ 0.9 were calculated; this gives an absorption coefficient $\alpha_i \cong 22 \sim 33$ 1/m.

Figure 2 shows sample results for radiation heat flux as a function of crank angle for a DI diesel engine at four different speeds.[6] Oguri and Inaba[12] described measurements made in diesel engines to obtain both the instantaneous radiation of heat transfer and its ratio to the total. Figure 3 shows radiation (surface) heat flux for two different speeds (revolutions per minute).

The radiant heat flux was extracted from the above-

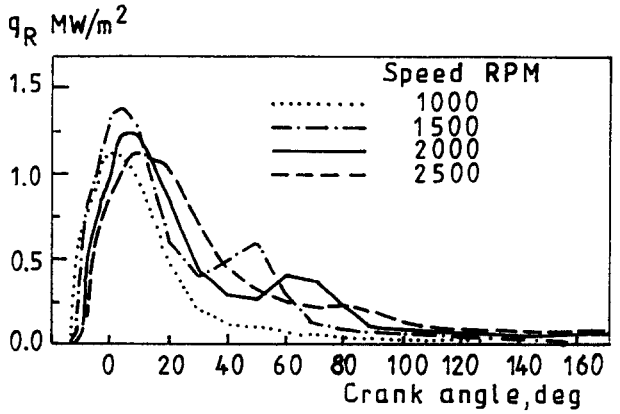

Figure 2 Apparent radiant heat flux when engine speed is varied[6]

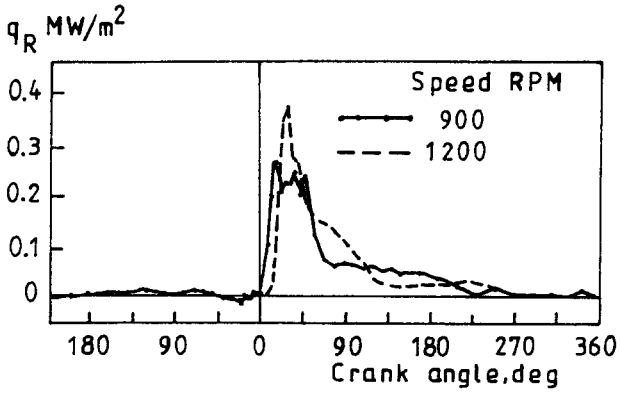

Figure 3 Surface radiant heat flux for two-speed variation[12]

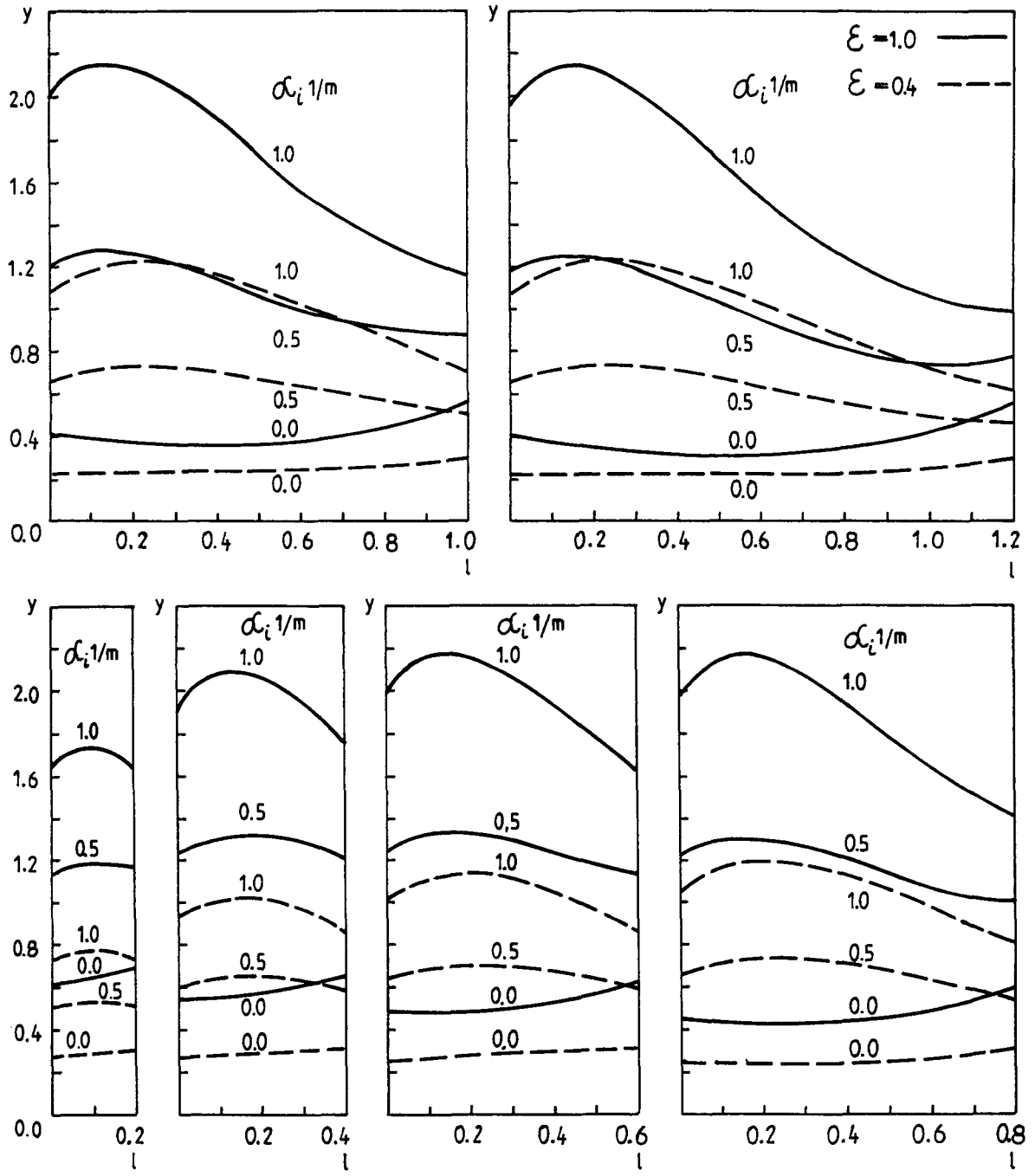

Figure 4 Variation (dimensionless) wall radiation heat flux distribution ($\alpha_i = 0.0$, 0.5, 1.0 and $\varepsilon = 0.4$, 1.0)

mentioned total flux by using a thermocouple covered with a sapphire window.[12] It will be noticed from Figures 2 and 3 that the experimental maximum value of q_R ranges from about 0.4–1.3 MW/m^2. This range is a consequence of the differing test conditions, and it will be seen below that predicted maximum values lie within this range.

Finally, the following variables affect the magnitude of the heat flux to the different surfaces of the engine combustion chamber and the temperature distribution in the components that comprise the chamber: engine speed, engine load, overall equivalence ratio, compression ratio, spark or injection timing, swirl and squish motion, mixture inlet temperature, coolant temperature and composition, wall material, and wall deposits. The comments that follow apply primarily to spark-ignition or compression-ignition and have been summarized by Heywood and Cohen.[8]

In the present study we have used a range of values of the parameters consistent with the quantitative results of experiments presented above. The analysis used appears satisfactorily to accommodate such a range of parameters.

For the temperature field inside the cylinder-piston system given in Table 1, calculations were carried out for the heat flux density $y(x)$ as a function of piston position l (related of course, to crank angle) varying from 0.2 (TDC) to 1.2 (BDC); these results are given in Figure 4. The effect of parametric variables other than piston position was also investigated, namely, dimensionless absorption k (0.00–0.1, i.e., values of $\alpha_i =$ 0.00–1.0 1/m), and surface emissivity $\varepsilon = 0.4$ and 1.0. When

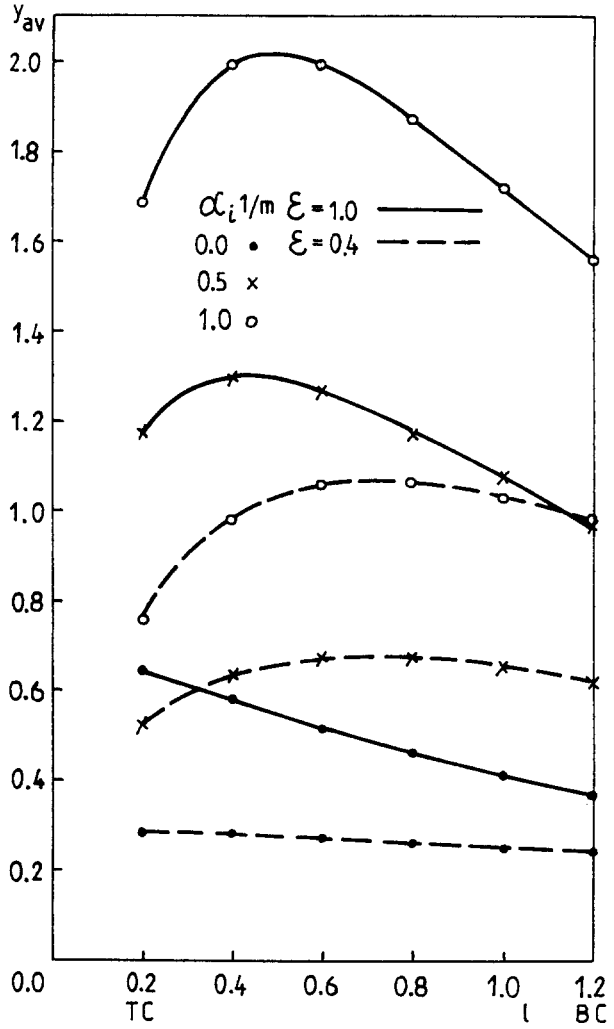

Figure 5 Average variation of (dimensionless) wall radiation heat flux distribution ($\alpha_i = 0.0$, 0.5, 1.0 and $\varepsilon = 0.4$, 1.0)

the wall emissivity is decreased the radiant heat flux decreases too. This is because, assuming equilibrium, reduced absorption means increased emission, hence more extraction of heat at the cylinder wall, hence less radiation.

Figures 5 and 6 give the (more customary) results for the mean heat flux density y_{av} as a function of the piston position, absorption coefficient ($\alpha_i = 1.0$; 15.0 and 20.0), and surface emissivity ($\varepsilon = 1.0$ and 0.2). The results obtained are both qualitatively and quantitatively compatible with values obtained experimentally.[1,3,6,8,12,25,28] The character and values of the dashed line (in Figure 6) are much the same as the curve in Figure 3 obtained experimentally by Oguri and Inaba.[12] For example, (1) for the case of $\alpha_i = 1.0$ 1/m ($k = 0.1$) the maximum value of y_{av} is 2.01 or in dimensional terms $q_R = 20{,}100$ W/m^2 (Figure 5), (2) for $\alpha_i = 20.0$ 1/m ($k = 0.2$) maximum is 24.0 or dimensionally $q_R = 240{,}000$ W/m^2 (Figure 6, point no. 5). However, the local radiation heat flux reached values of more than 300,000 W/m^2 during computation for $\alpha_i = 20.0$ 1/m and 403,000 W/m^2 for $\alpha_i = 30.0$ 1/m. These maximum values are quantitatively consistent with experimental data of Figure 3. Further confirmation is provided by Dent and Sulaiman,[3] whose piston-cylinder geometry was very close to that treated in this work. The radiation component of their measurements reached a maximum of around 300,000 W/m^2.

In order to check the accuracy of the analytical/numerical solution used, as well as the surface transformation concept for radiation gas bodies, the piston-cylinder system used for our example has also been solved by Hottel's zone method.[9–11] The results of these check calculations (for $\varepsilon = 1.0$) are presented in Figure 7. Additionally, one set of results obtained by the Monte Carlo method is presented in Figure 7 as well.[27] They show slight divergences in what are three approximate methods, although it is apparent that the Monte Carlo results and those obtained using the surface transformation methods are much closer near TDC. This is because the Hottel method in this region and along the liner is less accurate than the Monte Carlo method, but of course such an interpretation requires confirmation from additional Monte Carlo and Hottel data, which, it is hoped, will eventually become available. The novelty of this solution is in providing both local and temporal heat flux data, assuming instantaneous thermal equilibrium, and here an exponential distribution consistent with experiment.

Conclusions

A flexible and reliable analysis is presented for radiation heat transfer in an internal combustion engine cylinder. The Hottel zone and transformational zone methods have been used, together with treatment of gas radiation by elemental rings using Stasiek's principle of surface transformation. Results are

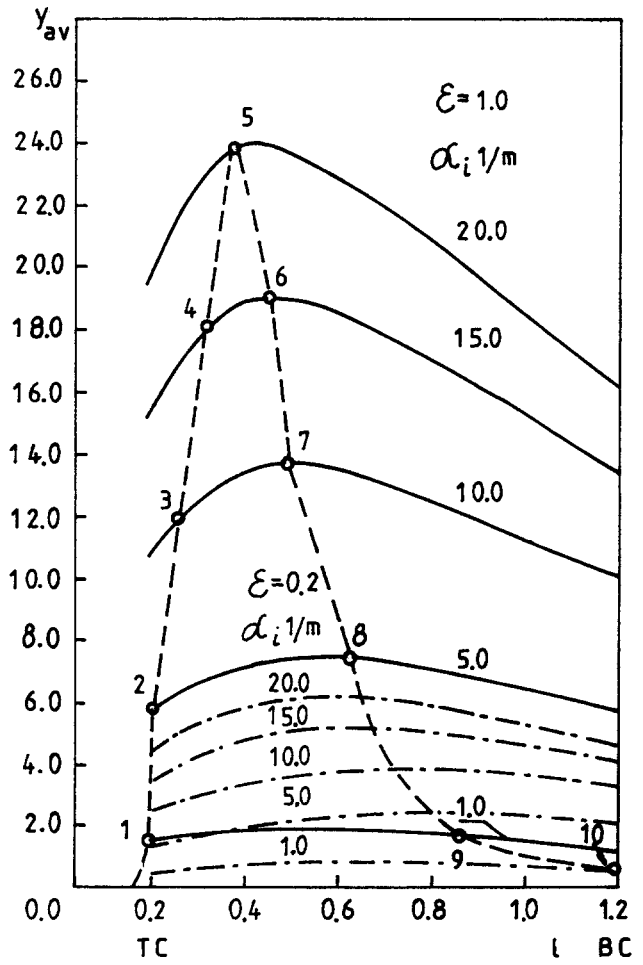

Figure 6 Average variation of (dimensionless) wall radiation heat flux distribution ($\alpha_i = 1.0$, 5.0, 10.0, 15.0, 20.0 and $\varepsilon = 1.0$). Dashed line was calculated in case variable parameter $\alpha_i = \alpha_i(l)$ (line 1-2-3-4-5-6-7-8-9-10)

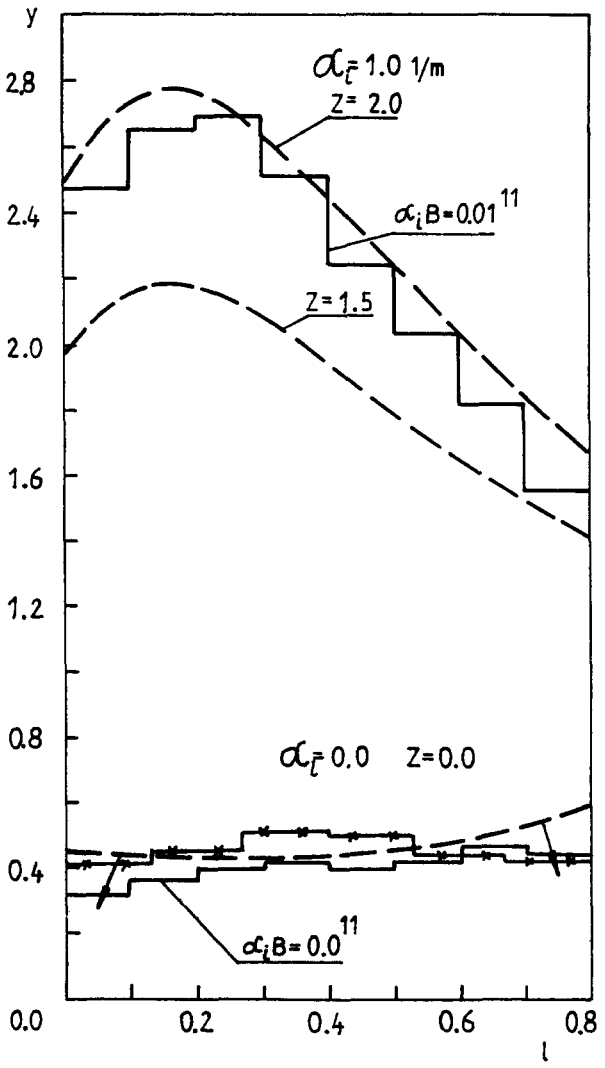

Figure 7 Comparison of transformational-zone (solid lines), Hottel-zone (dashed line), and Monte Carlo[27] methods

consistent with check predictions both using Hottel's method and a Monte Carlo approach.

For the system with a transparent medium ($\alpha = 0$) the solutions would have agreed more closely if the better approximations for configuration factors (as given by the first alternatives in Equations 38–42) were used. The exponential approximations actually used, namely the functions e^{-ax}, Equations 38–42, resulted in a surprisingly simple solution, however, although some inaccuracy has resulted.

It is worth stressing that the new method is relatively simple, less laborious, and more accurate than that of Hottel. Moreover, the solution is continuous. It is more adaptable, also, to being treated by computers or scientific calculators. Finally, the method can readily incorporate convective effects, and future work will address this issue.

Acknowledgment

We are very grateful to Dr. N. Verweyen of RWTH Aachen for supplying sample results of his Monte Carlo analysis.

References

1 Alkidas, A. C. and Myers, J. P. Transient heat-flux measurements in the combustion chamber of a spark-ignition engine. *J. Heat Transfer*, 1982, **104**, 62–67

2 Buraczewski, Cz. and Stasiek, J. Application of generalized Pythagoras theorem to calculation of configuration factors between surfaces of channels of revolution. *Int. J. Heat Fluid Flow*, 1983, **4**, 157–160

3 Dent, J. C. and Sulaiman, S. J. Convective and radiative heat transfer in a high swirl direct injection diesel engine. *Trans. S.A.E.*, 1978, **86**, 1758–1783

4 Edwards, D. K. and Balakrishnan, A. Thermal radiation by combustion gases. *Int. J. Heat Mass Transfer*, 1973, **16**, 25–40

5 Edwards, D. K. Molecular gas band radiation. *Advances in Heat Transfer*, vol. 12. Academic Press, New York, 1976, 115–193

6 Flynn, P., Mizusawa, M., Uyehara, O. A. and Myers, P. S. Determination of the instantaneous potential radiant heat transfer within an operating diesel engine. *Trans. S.A.E.*, 1972, **81**, 95–126

7 Gosman, A. D., Lockwood, F. C. and Salooja, A. P. The prediction of cylindrical furnaces gaseous fueled with premixed and diffusion burners. *Proc. 17th Int. Symposium on Combustion*, The Combustion Institute, Pittsburgh, PA, 1979, 747–760

8 Heywood, J. B. and Cohen, E. S. *Internal Combustion Engine Fundamentals*. McGraw-Hill, New York, 1988

9 Hottel, H. C. and Cohen, E. S. Radiant heat exchange in a gasfilled enclosure: Allowance for non-uniformity of gas temperature. *A.I.Ch.J.*, 1958, **4**, 2–14

10 Hottel, H. C. and Sarofim, A. F. The effect of gas flow patterns on radiative transfer in cylindrical furnaces. *Int. J. Heat Mass Transfer*, 1965, **8**, 1153–1169

11 Hottel, H. C. and Sarofim, A. F. *Radiative Transfer*. McGraw-Hill, New York, 1967

12 Oguri, T. and Inaba, S. Radiant heat transfer in diesel engines. *Trans. S.A.E.*, 1972, **81**, 127–147

13 Perlmutter, M. and Siegel, R. Heat transfer by combined forced convection and thermal radiation in heated tube. *J. Heat Transfer*, 1962, **84**, 302–311

14 Selcuk, N. and Siddall, R. G. Two-flux spherical harmonic modelling of two-dimensional radiative transfer in furnaces. *Int. J. Heat Mass Transfer*, 1976, **19**, 313–321

15 Siegel, R. and Howell, J. R. *Thermal Radiation Heat Transfer*. McGraw-Hill, New York, 1972

16 Sitkei, G. and Ramanaiah, G. V. A rotational approach for calculation of heat transfer in diesel engines. *Trans. S.A.E.*, 1972, **81**, 165–174

17 Smith, T. F., Shen, Z. F. and Alturki, A. M. Radiative and convective transfer in a cylindrical enclosure for a real gas. *ASME J. Heat Transfer*, 1985, **107**, 482–485

18 Smith, T. F., Shen, Z. F. and Friedman, J. N. Evaluation of coefficients for the weighted sum of gray gases model. *J. Heat Transfer*, 1982, **104**, 602–608

19 Clausen, C. W. and Smith, T. F. Radiative and convective transfer for real gas flow through a tube with specified wall heat flux. *J. Heat Transfer*, 1979, **101**, 376–378

20 Nakara, N. K. and Smith, T. F. Combined radiation-convection for a real gas. *J. Heat Transfer*, 1977, **99**, 60–65

21 Stasiek, J. Application of the generalized configuration factors and the principle of surface transformation to radiant heat exchange in system with optically active medium. *Z.N. P. G. Mechanika*, 1985, **49**, 1–116 (in Polish)

22 Stasiek, J. Transformational-zone method of calculation of complex heat exchange during flow of optically active medium inside tube of diffuse grey surface. *Wärme und Stoffübertragung*, 1988, **22**, 129–139

23 Stasiek, J. and Collins, M. W. Radiant and convective heat transfer for flow of an optically active gas in a cooled tube with a grey wall. *9th Int. Heat Transfer Conf.*, Jerusalem, Israel, August 19–24, 1990, **6**, 409–414

24 Tucker, R. J. Direct exchange areas for calculating radiation transfer in rectangular furnaces. *J. Heat Transfer*, 1986, **108**, 707–710

25 Wisniewski, S. Obciazenia cieplne silnikow tlokowych. Warszawa, W.K.L., 1972 (in Polish)

26 Horlock, J. H. and Winterbone, D. E. *The Thermodynamics and Gas Dynamics of Internal Combustion Engines*, Vol. II. Clarendon Press, Oxford, UK, 1986

27 Verweyen, N. Private communication, R. W. T. H. Aachen, Germany, 1988/1989

28 Woschni, G. and Fieger, J. Determination of local heat transfer coefficients at the piston of a high speed diesel engine by evaluation of measured temperature distribution. *Trans. SAE*, 1979, **88**, 2807–2815

29 Ozisik, M. N. *Radiative Transfer and Interactions with Conduction and Convection*. Wiley and Sons, New York, 1973

30 Poljak, G. Analysis of Heat Interchange by Radiation between Diffuse Surfaces. Tech. Phys. USSR, 1935, **1** (5–6), 555–590

Appendix 1: Angle (configuration) factor derivation

The four elementary configuration coefficients used in Equation 4 can be calculated by applying the differentiation of the known factors and the configuration factor algebra.[2,15]

In compliance with Figure 8 the equations for configuration coefficients are[1]

$$F_{1-2} = \frac{1}{2R_1^2}[R_1^2 + R_2^2 + X^2 - \sqrt{(R_1^2 + R_2^2 + X^2)^2 - 4R_1^2R_2^2}] \tag{33}$$

$$F_{d2-1} = \frac{X}{2R_2}\left[\frac{(R_1^2 + R_2^2 + X^2)}{\sqrt{[(R_1^2 + R_2^2 + X^2)^2 - 4R_1^2R_2^2]}} - 1\right] \tag{34}$$

for $R_1 = R_2 = R$

$$F_{d2-1} = \left[\frac{\frac{1}{2} + x^2}{\sqrt{(1 + x^2)}} - x\right] \cong \frac{e^{-2x}}{2} \tag{35}$$

where $x = X/D$.

As presented in Figure 8 the configuration between the elementary surface of the ring dA_2 and band A_i is

$$F_{d2-i} = F_i = F_{d2-1'} - F_{2-1} \tag{36}$$

or

$$F_{d2-i} = x\left[\frac{r_{1'}^2 + r_2^2 + x^2}{\sqrt{[(r_{1'}^2 + r_2^2 + x^2)^2 - 4r_{1'}^2 r_2^2]}} - \frac{r_1^2 + r_2^2 + x^2}{\sqrt{[(r_1^2 + r_2^2 + x^2)^2 - 4r_1^2r_2^2]}}\right] \tag{37}$$

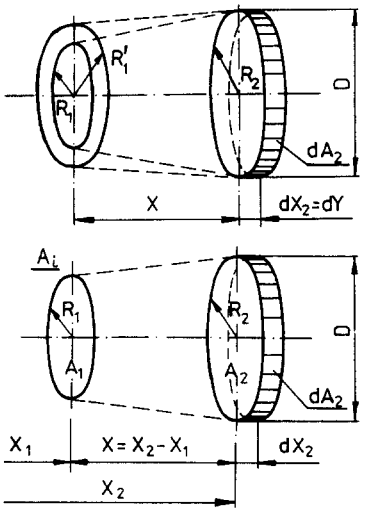

Figure 8 Geometry for calculation of configuration factors

where

$$r_i = \frac{R_i}{D}; \quad r_{1'} = \frac{R_{1'}}{D}; \quad r_2 = \frac{R_2}{D}; \quad x = \frac{X}{D}$$

In accordance with the dependence 37 and the calculation model adopted, the equations for the configuration coefficients become

$$F_{1,i} = F_{1,e} = x\left[\frac{0.26 + x^2}{\sqrt{[(0.26 + x^2)^2 - 0.01]}} - 1\right] \cong \frac{e^{-2x}}{32} \tag{38}$$

$$F_{2,i} = F_{2,e} = x\left[\frac{0.29 + x^2}{\sqrt{[(0.29 + x^2)^2 - 0.04]}} - \frac{0.26 + x^2}{\sqrt{[(0.26 + x^2)^2 - 0.01]}}\right] \cong \frac{e^{-2x}}{10} \tag{39}$$

$$F_{3,i} = F_{3,e} = x\left[\frac{0.34 + x^2}{\sqrt{[(0.34 + x^2)^2 - 0.09]}} - \frac{0.29 + x^2}{\sqrt{[(0.29 + x^2)^2 - 0.04]}}\right] \cong \frac{e^{-2x}}{8} \tag{40}$$

$$F_{4,i} = F_{4,e} = x\left[\frac{0.41 + x^2}{\sqrt{[(0.41 + x^2)^2 - 0.16]}} - \frac{0.34 + x^2}{\sqrt{[(0.34 + x^2)^2 - 0.09]}}\right] \cong \frac{e^{-2x}}{4} \tag{41}$$

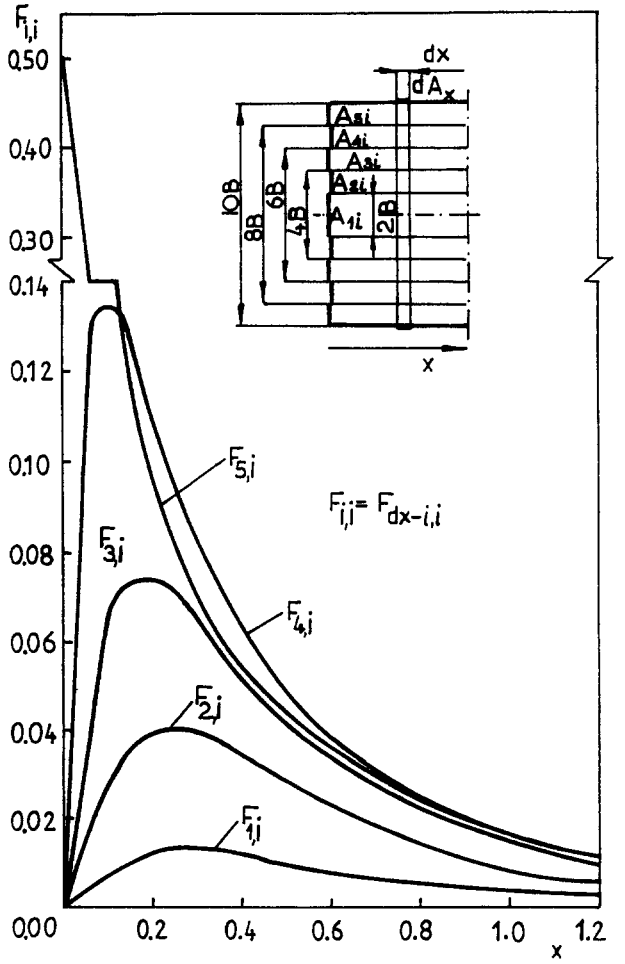

Figure 9 Configuration factors between a differential surface dA_x and circular strips

$$F_{5,i} = F_{5,e} = x\left[\frac{0.5 + x^2}{\sqrt{[(0.5 + x^2)^2 - 0.25]}} - \frac{0.41 + x^2}{\sqrt{[(0.41 + x^2)^2 - 0.16]}}\right] \cong \frac{e^{-2x}}{6} \quad (42)$$

These are shown in Figure 9 as functions of piston position x. The approximate values of the configuration coefficient in the form of exponential functions are correct for values of $x > 0.2$ and $B = 0.01$, as well as $D = 0.1$ m.

Appendix 2: Governing equations for zone method

The zone method consists of dividing an enclosure into a number of volume and surface zones where each zone is taken to be isothermal with uniform properties. The gas, then, is divided into volume zones with radial width $B = D/2i$ and axial length $H = L/j$, where i and j denote the number of radial and axial zones, respectively.

Once the total-exchange or directed-flux have been obtained for a gas enclosure, an energy conservation statement concerning each zone is made. This yields a set of equations that can be solved for the unknown temperatures and fluxes.

According to the Hottel zone method[9,10,15] and Figure 10, conservation of energy in the gas takes the form

$$H_i + R_i + H_{i,i} = H_{e,i} + Q_{h,i} + E_{bg,i} \quad (43)$$

or

$$\sum_{j=1}^{j=n} \overline{S_jG_i}e_{bj} + \sum_{j=1}^{j=m} \overline{G_jG_i}e_{bg,j} - 4\alpha_i V_i e_{bg,i} + \underbrace{\text{Net enthalpy flux into } i \text{ across its boundaries}}_{H_{i,i} - H_{e,i}} + \underbrace{\text{Net convective heat transfer from contiguous surface zones, if any}}_{Q_{h,i} = h_i A_i (T_{g,i} - T_{s,i})} + \frac{\text{combustion in zone } i}{H_i} = 0 \quad (44)$$

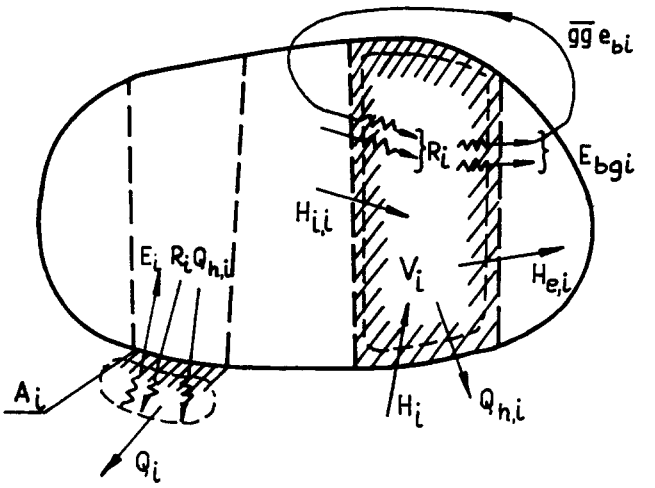

Figure 10 Heat flux densities of surface and volume elements for the Hottel zone method

The corresponding equation for a surface i is

$$R_i + Q_{h,i} = E_i + Q_i \quad (45)$$

or

$$Q_i = Q_{net,i} = \sum_{j=1}^{j=m} \overline{G_jS_i}e_{bj} + \sum_{j=1}^{j=n} \overline{S_jS_i}e_{bj} - A_i\varepsilon_i e_{bi} + h_iA_i(T_{g,i} - T_{s,i}) \quad (46)$$

where j includes i, and

$\overline{S_jS_i}$ = the surface–surface total exchange area
$\overline{S_jG_i}$ = the surface–gas total exchange area
$\overline{G_jG_i}$ = the gas–gas total exchange area

Hottel and Sarofim[10] show how matrix theory can be used as a computational tool in the zone method using total exchange area. In this paper the cylindrical and hence gas geometries are divided into voume and surface zones with dimensions $B = H = 0.01$ m.